Real-Time Model-Based Estimation of SOC and SOH for Energy Storage Systems

Mario Cacciato, *Member, IEEE*, Giovanni Nobile, Giuseppe Scarcella, *Member, IEEE*, and Giacomo Scelba, *Member, IEEE*

***Abstract*—To obtain a full exploitation of battery potential in energy storage applications, an accurate modeling of electrochemical batteries is needed. In real terms, an accurate knowledge of state of charge (SOC) and state of health (SOH) of the battery pack is needed to allow a precise design of the control algorithms for energy storage systems (ESSs). Initially, a review of effective methods for SOC and SOH assessment has been performed with the aim to analyze pros and cons of standard methods. Then, as the trade-off between accuracy and complexity of the model is the major concern, a novel technique for SOC and SOH estimation has been proposed. It is based on the development of a battery circuit model and on a procedure for setting the model parameters. Such a procedure performs a real-time comparison between measured and calculated values of the battery voltage while a PI-based observer is used to provide the SOC and SOH actual values. This ensures a good accuracy in a wide range of operating conditions. Moreover, a simple start-up identification process is required based on battery data-sheet exploitation. Because of the low computational burden of the whole algorithm, it can be easily implemented in low-cost control units. An experimental comparison between SOC and SOH estimation performed by suggested and standard methods is able to confirm the consistency of the proposed approach.**

***Index Terms*—Adaptive algorithms, energy storage systems modeling, runtime model, state of charge, state of health.**

NOMENCLATURE

BMS	Battery management system.
C_n	Rated capacity (Ah).
C1	Nominal capacity, discharge time 1 h (Ah).
C20	nominal capacity, discharge time 20 h (Ah).
Q	Coulomb charge (As).
EKF	Extended Kalman filter.
$v(t)$	Measured battery voltage (V).
$i(t)$	Battery current (A), positive during discharge.
T	Temperature (°C).
VRLA	Valve-regulated lead acid battery.
Li-ion	Lithium ions battery.
Ni-MH	Nickel metal hydride.

Manuscript received July 13, 2015; revised January 12, 2016 and October 26, 2015; accepted February 19, 2016. Date of publication February 26, 2016; date of current version September 16, 2016. This work was supported in part by the Research Project "PON02_153_2939517 Tecnologie ad alta Efficienza per la Sostenibilità Energetica ed ambientale On-board—TESEO." Recommended for publication by Associate Editor M. Ferdowsi.

The authors are with the Department of Electrical, Electronics Engineering, and Computer Science, University of Catania, I-95125 Catania, Italy (e-mail: mario.cacciato@dieei.unict.it; giovanni.nobile@unict.it; giuseppe.scarcella@dieei.unict.it; giacomo.scelba@dieei.unict.it).

Color versions of one or more of the figures in this paper are available online at http://ieeexplore.ieee.org.

Digital Object Identifier 10.1109/TPEL.2016.2535321

I. INTRODUCTION

IN recent years, addressing smart-grid applications such as renewable energy power plants and plug-in electric vehicles, energy storage system (ESS) based on electrochemical batteries have been extensively studied and used, playing a key role in resources exploitation as well as energy consumption optimization [1], [2].

Availability of an accurate model of ESS is essential for control strategy optimization in power electronics systems. This is also aimed at obtaining the maximum energy recovery and extend battery lifetime. The ESS operation can be modeled in many different ways: a first important category is represented by electrochemical models using the equations governing the physicochemical phenomena occurring in a battery [3], [4]. The implementation of these models involves a specialized knowledge on electrochemistry, hence their exploitation in the field of electrical and electronics engineering is rare. Instead, the models based on equivalent electrical circuit become the most suitable choice because of their simple implementation in popular simulation tools. Also, they can be easily integrated in control algorithms of battery management systems (BMS).

To properly describe ESS operations, a consistent number of suitable equivalent electrical circuits have been reported in literature [5]–[8]. In general, the basic battery models are based on the connection in series of a constant voltage generator and a resistor [6], [7], [9], [10]. The generator represents the no-load voltage E_0, i.e., the electrical potential at battery terminals without load, while the resistor takes into account the voltage drop related to internal and terminals resistance. The approaches of Sheperd, Unnewehr, and Nernst improve the voltage value prediction provided by the previous simple models by adding one or more controlled voltage sources set by state-of-charge (SOC) values [5], [11]–[13]. In the so-called "*RC* linear models," series *RC* elements are added in the circuit to better track voltage transients during current steps [5], [7], [9], [11], [14]–[18]. These models also reproduce the dependency of E_0 from the SOC of the battery. In parameter-varying models, more complex circuits are introduced in order to obtain a good accuracy both in dynamic conditions and for battery operation in the long term [7], [9], [19]–[29]. In such a case, the values assigned to some of the circuit parameters cannot be considered as constants since they depend on the actual SOC and state of health (SOH) and on the external conditions such as imposed current rate, working temperature, and so on. Other more sophisticated models are used to reproduce the ESS operation in particular applications (e.g., charge of lead-acid batteries in stand-alone photovoltaic plants)

or specific phenomena (e.g., temperature effect) and therefore their use is limited to specific cases [10], [30]–[33].

According to the previous analysis, the accurate estimation of SOC and SOH is a key issue to properly reproduce ESS operation. In the aforementioned demanding applications where ESS nonlinearity becomes relevant, the current counting method used as standard algorithm to estimate SOC shows significant limits [10], [38]–[40]:

1) accurate knowledge of initial value of SOC and actual capacity are needed;
2) measurement errors lead to wrong estimation due to the integral calculation;
3) current acquisition must be performed continuously.

In order to overcome such drawbacks, alternative and more advanced methods have been proposed and some of them also perform a continuous SOH estimation [39], [40]. Basically, full discharge test methods described in [39], [41], and [42] are normally used to estimate the SOC and SOH of a ESS by forcing a full discharge while the charge is counted until the battery terminal voltage reaches the "end of discharge voltage" value provided by the manufacturer. The current shall be maintained at a constant value during the discharge. To properly operate the procedure, the battery must be fully charged before the test and a temperature compensation technique is required. Open circuit voltage methods are based on the measurement of no-load curve SOC(E_0) that can be defined for each ESS. The main drawback is represented by the long period of time necessary to reach the final relaxation voltage E_0 after a charge or discharge [17], [40], [43], [44]. An improvement can be obtained by exploiting terminal voltage analysis methods, which analyze the voltage waveform in both charge and discharge operations, i.e., these kind of methods can be easily implemented online [40], [45], [46]. In such circumstances, the accuracy is strongly affected by the current rate (e.g., Peukert effect) and environmental conditions (e.g., working temperature).

Impedance methods are based on a different approach because ESS models work with internal impedance at different frequencies identified by analyzing the response to the pulsed current test [31], [39], [40], [46]–[48]. This class of methods ensures good accuracy, but it can often be too sensitive to measurement noise. More advanced methods have been developed from evolutionary computing including genetic algorithms, neural networks, fuzzy logic, and so on [3], [40], [48]. In such an instance, great accuracy can be obtained only if a big computational burden can be accepted. A significant reduction in the amount of training data can be obtained by applying current pulse response methods [38], [49]. These perform the SOC and SOH estimation from the analysis of the terminal voltage waveform when ESS is forced by a predefined low-frequency pulsed current. The implementation of these methods requires some preliminary experimental tests necessary to map the expected ESS behavior. In doing so, the accuracy strongly decreases if actual operating points differ from the predefined ones. The methods based on Kalman Filter and observers (sliding-mode observer, Luenberger observer, PI-based observer, etc.) represent other classes suitable for accurate ESS estimation. Their implementation can be easily matched with parameter-varying circuit models with a significant noise rejection [26]–[29], [50]–[56]. In several applications, observer-based methods can ensure good precision and an acceptable computational burden. Finally, another class represented by hybrid methods properly merges the previous methods while overcoming their limitations, especially during prolonged ESS operation [57]–[60].

It is important to consider that neither models nor methods are able to fulfill the performance required by demanding applications. Therefore, the selection of the appropriate algorithm is up to the designer, mainly depending on his or her knowledge of the addressed application. To this aim, the information provided earlier can help in choosing the best approach. Among circuit models, the runtime-based ones classified into parameter-varying models category can be considered a good compromise between performance and complexity [61].

Starting from such a category, a novel SOC and SOH estimation method has been developed. In particular, the combination of a modified version of the circuit model described in [21] and a PI-based observer approach is used to correctly estimate battery dynamic as well as SOC and SOH. The result is a flexible method able to ensure a good accuracy with a low computational burden, allowing its easy implementation in low-cost control units. Furthermore, the proposed method requires some preliminary operations for model initialization, based on simple measurements.

PI controllers are used in the observers as an effective solution to yield the estimation method suitable for several battery technologies and applications by means of a simple PI tuning procedure. Effective examples of PI-based observers used in ESS state estimation are in [54] and [55]. In [54], battery is modeled by the Thevenin equivalent circuit described in [7], [9], and [11]. This kind of model allows for simple implementation but can lead to large errors if the operating conditions differ from the rated ones. A single *RC* network is included to track dynamic behavior, i.e., ESS can be properly modeled only within a limited frequency range. No information about actual SOH is available. In [55], the proposed SOC estimation method is a combination of an open-loop current integrator and a PI-based observer. It also uses a drifting current corrector to restrain the influence of the drifting current. In several cases, due to the mixed methods, the implementation of the entire algorithm could be too expensive from a computational point of view. Again, no information about SOH is provided.

Finally, the main difference between the algorithm proposed in this paper and other works in literature including PIs, is the exploitation of an advanced parameter-varying circuit model whose parameters are tuned in real time by the proposed PI-based observer. The analysis of circuit parameters variation during battery operation leads to SOC and SOH simultaneous estimation by means of simple formulas. This is also the case in variable working conditions.

II. Model-Based Estimation of SOC and SOH

The proposed battery model, shown in Fig. 1, is derived from the circuit model described in [21]. An additional resistive element $R_{\rm cap}$ has been connected in series with $C_{\rm cap}$. The voltage

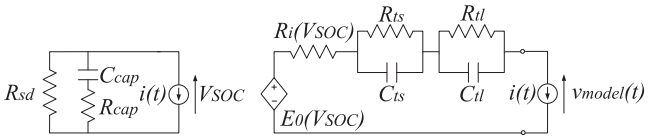

Fig. 1. Proposed circuit model.

drop associated to $R_{\rm cap}$ allows to better represent the reduction of the ESS capacity at high currents, known as Peukert effect [35]. Moreover, to take into account the variation of internal resistance with actual SOC, R_i value is related to the voltage $V_{\rm SOC}$ [9], [37]. The voltage $V_{\rm SOC}$ is the SOC value expressed in terms of voltage variation at the terminals of the series $C_{\rm cap} - R_{\rm cap}$, multiplied by a factor 100.

The parameters $R_{\rm ts}$, $C_{\rm ts}$, $R_{\rm tl}$, and $C_{\rm tl}$ are used to describe the ESS dynamic behavior. Their values can be easily determined, as described in [16], by performing simple preliminary tests and then by analyzing the voltage waveform during current steps. The modification of the value of these parameters during battery operation can be often neglected. This assumption leads to significant model complexity reduction while maintaining good accuracy. Whenever the operating conditions of ESS considerably differ from the rated ones, the tuning of the circuit parameters can be easily performed as described in [16] and [21]. The circuit model can be simulated by considering its state-space representation where the capacitors voltages $v_{C_{\rm ts}}, v_{C_{\rm tl}}$, and $v_{\rm cap}$ are the state variables, as in (1). The current and terminal voltage are considered the input and output variables, respectively

$$\begin{bmatrix} \dot{v}_{C_{\rm ts}} \\ \dot{v}_{C_{\rm tl}} \\ \dot{v}_{C_{\rm cap}} \end{bmatrix} = \begin{bmatrix} -\dfrac{1}{R_{\rm ts}C_{\rm ts}} & 0 & 0 \\ 0 & -\dfrac{1}{R_{\rm tl}C_{\rm tl}} & 0 \\ 0 & 0 & A_{33} \end{bmatrix} \cdot \begin{bmatrix} v_{C\rm ts} \\ v_{C\rm tl} \\ v_{C\rm cap} \end{bmatrix} + \begin{bmatrix} \dfrac{1}{C_{\rm ts}} \\ \dfrac{1}{C_{\rm tl}} \\ B_{31} \end{bmatrix} \cdot i$$

$$v_{\rm model} = \begin{bmatrix} -1 & -1 & C_{13} \end{bmatrix} \cdot \begin{bmatrix} v_{C_{\rm ts}} \\ v_{C_{\rm tl}} \\ v_{C_{\rm cap}} \end{bmatrix} + D \cdot i + n \tag{1}$$

where

$$\begin{aligned} A_{33} &= -\frac{1}{C_{\rm cap}\left(R_{\rm sd} - R_{\rm cap}\right)} B_{31} = \frac{R_{\rm sd}}{C_{\rm cap}(R_{\rm sd} - R_{\rm cap})} \\ C_{13} &= m\left(\frac{R_{\rm sd}}{R_{\rm sd} - R_{\rm cap}}\right) D = -R_i - R_{\rm cap}C_{13} \\ E_0 &= m \cdot V_{\rm SOC} + n. \end{aligned} \tag{2}$$

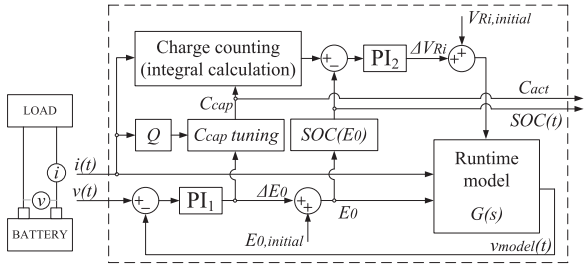

Fig. 2. Proposed real-time SOC and SOH estimation scheme.

The constants m and n are used for linear approximation of E_0 ($V_{\rm SOC}$), as well as E_0(SOC) relationship. Such an assumption can be coarse for some kind of Li-ion batteries [43], [60]. In such a case, different curve-fitting methods or polynomial expressions can be used [54]. Transfer function $G(s)$ of the aforementioned representation in s-domain is given by

$$\begin{aligned} G(s) &= \frac{\rm num(s)}{\rm den(s)} + D \\ {\rm num}(s) &= {\rm num1}(s) + {\rm num2}(s) + {\rm num3}(s) \\ {\rm den}(s) &= \left(s + \frac{1}{R_{\rm ts}C_{\rm ts}}\right)\left(s + \frac{1}{R_{\rm tl}C_{\rm tl}}\right)(s - A_{33}) \end{aligned} \tag{3}$$

where

$$\begin{aligned} {\rm num1}(s) &= -\frac{1}{C_{\rm ts}}\left(s + \frac{1}{R_{\rm tl}C_{\rm tl}}\right)(s - A_{33}) \\ {\rm num2}(s) &= -\frac{1}{C_{\rm tl}}\left(s + \frac{1}{R_{\rm ts}C_{\rm ts}}\right)(s - A_{33}) \\ {\rm num3}(s) &= C_{13}B_{31}\left(s + \frac{1}{R_{\rm ts}C_{\rm ts}}\right)\left(s + \frac{1}{R_{\rm tl}C_{\rm tl}}\right). \end{aligned} \tag{4}$$

SOC and SOH are evaluated by using the PI-based estimation scheme shown in Fig. 2 that includes the circuit model of Fig. 1. During the operation of the ESS, the algorithm acquires voltage $v(t)$ and current $i(t)$. Then, $v(t)$ is compared to the value provided by the circuit model $v_{\rm model}(t)$ and amplified by the $\rm PI_1$ controller, providing a correction term ΔE_0, which is used to estimate the no-load voltage E_0. This quantity is used to estimate the SOC by using the relationship SOC(E_0), usually provided by data sheets. If the actual working temperature is quite different from the expected one, it is recommended to define SOC(E_0) curves at different temperatures [54], [60]. In practice, these curves can be included in SOC(E_0) block in Fig. 2, by using a look-up table with two inputs E_0 and T. Therefore, SOC(E_0) is compared to the value obtained by the charge counting relationship (5), the error is amplified by the $\rm PI_2$ controller and the output ΔV_{R_i} is used as a correction factor of the model output during charge and discharge (not-zero current operation). ΔV_{R_i} represents the increment of the internal resistance R_i at low SOC values [9], [37]

$${\rm SOC}(t) = {\rm SOC}(t_0) - \frac{1}{C_{\rm cap}} \cdot \int_{t_0}^{t} i(t)dt. \tag{5}$$

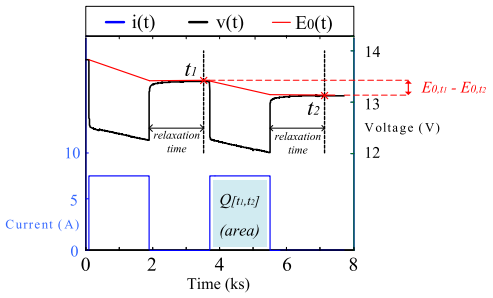

Fig. 3. Identification of voltage drop ΔE_0 due to a pulsed discharge.

In the proposed method, $C_{\rm cap}$ is continuously updated and its actual value is provided by the block $C_{\rm cap}$ *tuning* of Fig. 2. From the basic formulation of the electrical capacitance, $C_{\rm cap}$ is generally expressed in (6) where the charge Q and the no-load voltage drop ΔE_0, related to $V_{\rm SOC}$ by (2), are evaluated during a single or a sequence of charge–discharge operations. Also, in (6), SOH calculation is expressed as the ratio of the actual $C_{\rm cap}$ to the rated capacity C_n

$$C_{\rm cap} = f[Q(i(t)), \Delta E_0(t)]{\rm SOH} = \frac{C_{\rm cap}}{C_n}. \tag{6}$$

More precisely, $C_{\rm cap}$ value can be calculated as the ratio of the charge Q removed (stored) during a discharge (recharge) to the variation of voltage $V_{\rm SOC}(t)$, related to E_0 by (2), caused by the discharge (recharge) [18], [27]. Although Q can be simply calculated from (7), being the time integral of the current during a period $t = [t_1, t_2]$, $\Delta E_0(t)$ cannot be evaluated by simply measuring $v(t)$ due to its large relaxation time, as shown in Fig. 3

$$Q_{[t_1,t_2]} = \int_{t_1}^{t_2} i(t)dt. \tag{7}$$

As the proposed method solves this problem by performing a continuous estimation of E_0, related to $V_{\rm SOC}$ by (2), even during charge or discharge of the ESS, $C_{\rm cap}$ can be estimated in real time with no delay using (8)

$$C_{\rm cap} = \frac{Q_{[t_1,t_2]}}{V_{{\rm SOC},t_1} - V_{{\rm SOC},t_2}} = \frac{m \cdot Q_{[t_1,t_2]}}{E_{0,t_1} - E_{0,t_2}}. \tag{8}$$

Whenever the proposed scheme is applied, ESS state is updated in terms of SOC and SOH estimation while the parameters of the equivalent circuit are properly settled. In order to increase the estimation accuracy, data from several discharge operations are averaged.

Preliminary coarse tuning for PI controllers can be achieved in a simple but effective way by exploiting the transfer function of the estimation scheme and alternatively considering two subsystems, each one related to a single PI controller. Suitable approximations can be considered, such as:

1) analysis is performed on fixed operating points; consequently, some variables and circuit parameters are assumed as constants;
2) due to the previous statement and from appropriate selection of control variables and input for subsystems, reciprocal interaction between controllers can be neglected;
3) subsystems transfer functions can be simplified in case of dominant poles;
4) closed-loop subsystems can be approximated with second-order transfer functions.

Tuning procedure is performed by using an analytical approach. Accordingly, PI gains are calculated in order to obtain specific closed-loop subsystem poles. Optimal position of these poles, named p_a and p_b, is calculated from design requirements assigned to voltage waveform during transients.

Referring to $\rm PI_1$ and its closed-loop subsystem, E_0(SOC) represents the control variable while its dynamics is mainly affected by $C_{\rm cap}, R_{\rm cap}$, and $R_{\rm sd}$ parameters related to $V_{\rm SOC}$ variation. The closed-loop transfer function is given by (9) where G_{c1} is referred to the PI controller, G_{ss1} is the plant transfer function derived from the circuit model taking into account the approximations mentioned earlier

$$\begin{aligned} G_{cl1} &= \frac{G_{c1}G_{ss1}}{1 + G_{c1}G_{ss1}} G_{c1} = kp_1 + \frac{ki_1}{s} \\ G_{ss1} &\cong R_\alpha + \frac{mR_{\rm sd}^2}{C_{\rm cap}R_\beta^2\,(s - (1/C_{\rm cap}R_\beta))} \\ R_\alpha &= \frac{mR_{\rm cap}R_{\rm sd}}{R_\beta} - R_i R_\beta = R_{\rm cap} - R_{\rm sd}. \end{aligned} \tag{9}$$

Considering V_{R_i} as control variable, a similar analysis can be performed for $\rm PI_2$. In such a case, system dynamic is mainly affected by $C_{\rm tl}$ and $R_{\rm tl}$ parameters related to voltage response during current step. Referring to a specific operating point, E_0(SOC) can be treated as a constant input. From the described analytical formulation, gains *kp* and *ki* for each PI are calculated as algebraic solutions of the linear systems:

$$\begin{cases} \dfrac{mkp_1R_{\rm sd}^2 + ki_1R_\alpha R_\beta^2 C_{\rm cap} - kp_1R_\alpha R_\beta - R_\beta}{kp_1R_\alpha R_\beta^2 C_{\rm cap} + R_\beta^2 C_{\rm cap}} = p_{a1} + p_{b1} \\ \dfrac{mki_1R_{\rm sd}^2 - ki_1R_\alpha R_\beta}{kp_1R_\alpha R_\beta^2 C_{\rm cap} + R_\beta^2 C_{\rm cap}} = p_{a1}p_{b1} \end{cases}$$

$$\begin{cases} \dfrac{kp_2(R_{\rm tl}/R_i) + kp_2 + ki_2C_{\rm tl}R_{\rm tl} - 1}{kp_2C_{\rm tl}R_{\rm tl} - C_{\rm tl}R_{\rm tl}} = p_{a2} + p_{b2} \\ \dfrac{ki_2(R_{\rm tl}/R_i) + ki_2}{kp_2C_{\rm tl}R_{\rm tl} - C_{\rm tl}R_{\rm tl}} = p_{a2}p_{b2}. \end{cases} \tag{10}$$

The observability and stability analysis behind the proposed method has been performed by considering the same approximations used for PI tuning. Again, the estimation scheme shown in Fig. 2 can be divided into two separate subsystems, each one including a single PI observer. Hence, reciprocal interaction between controllers has been neglected in the following analysis.

The observability and stability have been evaluated by using an approach similar to that described in [54]. In particular, the first step is to assess the observability, i.e., to establish if the estimation scheme is able to determine the ESS states from the observation of the output over a certain time interval. From the state-space representation of the battery circuit model, the observability matrix has to be calculated and analyzed: if such a matrix is always full rank under any operating condition, the

battery model is observable and it is possible to estimate the internal state.

The second step is to assess stability by considering the state-space representation of a generic observer system, including PI [54]

$$\begin{cases} \dot{\hat{x}} = A\hat{x} + Bu + kp_i\,(y - \hat{y}) + w \\ \dot{w} = ki_i\,(y - \hat{y}) \end{cases} \tag{11}$$

where *w* is the integral of the difference between the measured output y and the output provided by the observer $\hat{y}$. The observer error is defined by

$$\tilde{e} = \hat{x} - x. \tag{12}$$

so that

$$\begin{cases} \dot{\tilde{e}} = A\tilde{e} - kp_i C\tilde{e} + w \\ \dot{w} = -ki_i C\tilde{e} \end{cases} \mapsto \begin{pmatrix} \dot{\tilde{e}} \\ \dot{w} \end{pmatrix} = A_e \begin{pmatrix} \tilde{e} \\ w \end{pmatrix}. \tag{13}$$

Therefore, the observer dynamics is governed by matrix A_e

$$A_e = \begin{bmatrix} A - kp_i C & 1 \\ -ki_i C & 0 \end{bmatrix}. \tag{14}$$

Since observability has been previously proved, PI gains can be properly assigned in order to ensure A_e is a Hurwitz matrix, which means that the observer system would asymptotically converge, i.e., the estimated states would asymptotically converge to the true states.

Finally, in order to comply with both PI tuning procedures described earlier and stability requirements, it has to be verified that PI gains calculated as algebraic solutions of the linear systems (10) ensure observability and stability under any operating condition.

Referring to the subsystem whose controller is PI_1, the ESS state-space representation matrices can be calculated from plant transfer function G_{ss1} (9), obtaining

$$\begin{aligned} A &= -\frac{1}{C_{\mathrm{cap}}\,(R_{\mathrm{sd}} - R_{\mathrm{cap}})} B = \frac{R_{\mathrm{sd}}}{C_{\mathrm{cap}}(R_{\mathrm{sd}} - R_{\mathrm{cap}})} \\ C &= m\left(\frac{R_{\mathrm{sd}}}{R_{\mathrm{sd}} - R_{\mathrm{cap}}}\right) D = -R_i - m\left(\frac{R_{\mathrm{sd}}}{R_{\mathrm{sd}} - R_{\mathrm{cap}}}\right). \end{aligned} \tag{15}$$

The observability matrix is given by

$$O_1 = \begin{bmatrix} C \\ CA \end{bmatrix} = \begin{bmatrix} \dfrac{mR_{\mathrm{sd}}}{R_{\mathrm{sd}} - R_{\mathrm{cap}}} \\ -\dfrac{mR_{\mathrm{sd}}}{C_{\mathrm{cap}}(R_{\mathrm{sd}} - R_{\mathrm{cap}})^2} \end{bmatrix}. \tag{16}$$

It can be stated that the observability matrix is always full rank because under no circumstance, a linear dependence between rows can be recognized. The battery model is observable under any operating condition, i.e., it is possible to estimate the internal state of the battery.

To assess stability for the subsystem whose controller is PI_1, the matrix A_e must be analyzed. This can be easily calculated by (14)

$$A_{e1} = \begin{bmatrix} -\dfrac{1}{C_{\mathrm{cap}}\,(R_{\mathrm{sd}} - R_{\mathrm{cap}})} - kp_1 \dfrac{mR_{\mathrm{sd}}}{R_{\mathrm{sd}} - R_{\mathrm{cap}}} & 1 \\ -ki_1 \dfrac{mR_{\mathrm{sd}}}{R_{\mathrm{sd}} - R_{\mathrm{cap}}} & 0 \end{bmatrix}. \tag{17}$$

Since observability has been previously proved, kp_1 and ki_1 can be assigned in order to ensure A_{e1} is a Hurwitz matrix: in this way, the estimation states asymptotically converge to the true states. During experimental testing of the proposed method, it has been verified that tuning of PI_1, performed accordingly to (10), satisfies the stability criterion described here.

A similar analysis can be performed for the subsystem whose controller is PI_2. By repeating the same procedure used for the subsystem including PI_1, the observability matrix can be easily calculated

$$O_2 = \begin{bmatrix} C \\ CA \end{bmatrix} = \begin{bmatrix} -1 \\ \dfrac{1}{C_{\mathrm{tl}} R_{\mathrm{tl}}} \end{bmatrix}. \tag{18}$$

Once again, it can be stated that the observability matrix is always full rank because under no circumstance a linear dependence between rows can be recognized. Therefore, the battery model is observable. From (14), the matrix A_{e2} governing observer dynamics can be easily determined

$$A_{e2} = \begin{bmatrix} -\dfrac{1}{C_{\mathrm{tl}} R_{\mathrm{tl}}} + kp_2 & 1 \\ ki_2 & 0 \end{bmatrix}. \tag{19}$$

Since observability has been previously proved, kp_2 and ki_2 can be assigned in order to ensure A_{e2} is a Hurwitz matrix, i.e., the estimation states asymptotically converge to the true states. It was experimentally verified that tuning of PI_2 performed according to (10) satisfies the stability requirements under any operating condition.

TABLE I
BATTERIES USED FOR EXPERIMENTAL SETUP

ID	Technology	Nominal Voltage (V)	Nominal Capacity (Ah)
Battery 1	VRLA	12	7.2 (C20)
Battery 2	VRLA	12	27 (C20)
Battery 3	Li-ion	51.2	40 (C1)
Battery 4	Ni-MH	12	4.8 (C20)

III. EXPERIMENTAL VALIDATION

Performance of the proposed estimation method has been experimentally validated by using VRLA and Li-ion and Ni-MH batteries whose technical specifications are listed in Table I.

The effectiveness of the proposed approach has been proven by analyzing the results of experimental tests in terms of estimation accuracy and computational effort in comparison to EKF. EKF represents one of the most commonly used approaches in the context of battery estimation due to several inherent advantages such as the adaptability to nonlinear systems, compensation for inaccuracies in model, and measurements and ability to

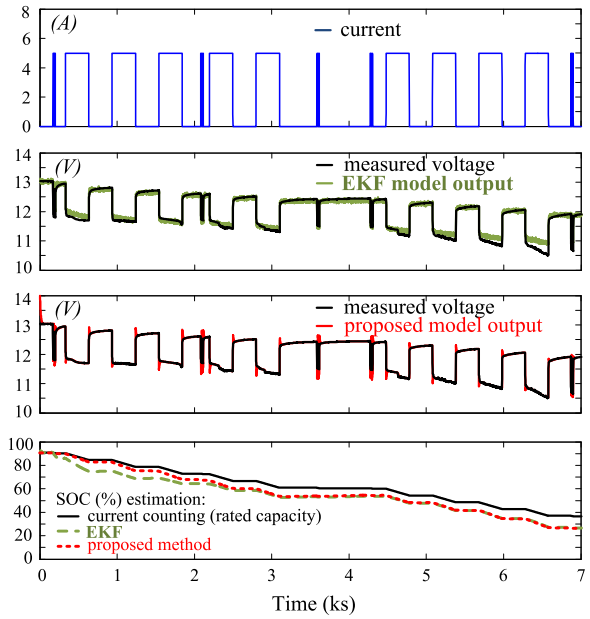

Fig. 4. Experimental tests performed with battery 1, VRLA 12V 7.2 Ah, working temperature 20 °C. Comparison between EKF and proposed method used for SOC estimation during discharge operation. Estimated SOH is about 83% in both cases.

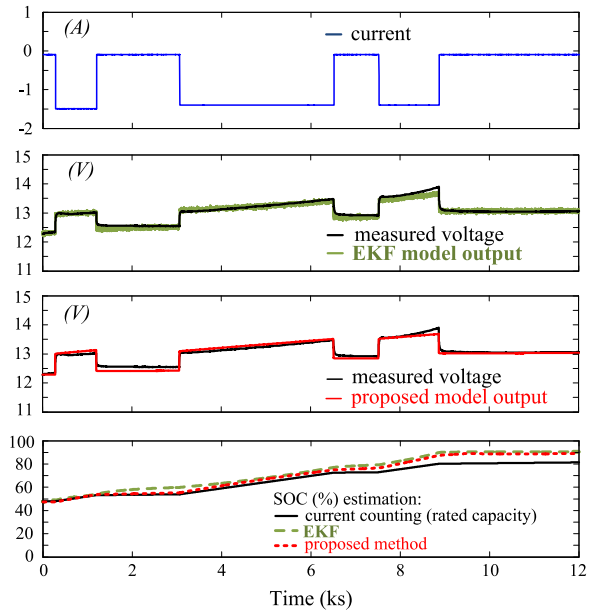

Fig. 5. Experimental tests performed with battery 1, VRLA 12 V 7.2 Ah, working temperature 20 °C. Comparison between EKF and proposed method used for SOC estimation during charge operation. Estimated SOH is about 83% in both cases.

track changes in circuit parameters [26]–[29]. The selected EKF algorithm has been implemented, as described in [27]. The tuning of PI controllers has been performed by applying (10). Due to the slow dynamic behavior observed during current steps for the batteries listed in Table I, a preliminary coarse assignment leads to values typically around 0.1 for kp_1 and kp_2 and around 1 for ki_1 and ki_2. However, a fine-tuning is highly recommended for each battery considering the actual operating scenario.

Fig. 4 shows the current, measured and estimated voltages, and SOC during a random discharging sequence applied to battery 1 at a working temperature of 20 °C. The result confirms that SOC estimation performed by the proposed method matches the one provided via EKF in long term. As an advantage, the relevant initial settling time showed for EKF due to its recursive procedure has been largely reduced, as it can be noted on the initial SOC responses of the last plot in Fig. 4. Moreover, the profiles of SOC highlight the ability of the estimation algorithms to consider SOH. In fact, the current counting in its basic implementation totally neglects the ageing, i.e., the SOH value is equal to 100% and the related SOC profile deviates to wrong values, while on the contrary, the other two methods converge. Similar results are obtained during a sequence of charge operations, as shown in Fig. 5.

Consistency of the proposed approach is confirmed but achievable accuracy is typically lower in comparison to discharge operation, as expected. Indeed, modeling of ESS behavior during charge is typically more complicated due to well-known additional phenomena, as reported in [5], [21], and [24]. Circuit model tuning during charge operations leads to increased values of internal resistance R_i, as expected [5].

The estimation of actual SOH for battery 1 has been performed during the experimental tests: the estimation carried out by applying the proposed method is close to that provided by EKF and by the IEEE standard 1188-2005 full-discharge test [41], [42], as shown in Table II. The implementation of the IEEE standard 1188-2005 is shown in Fig. 6. In this analysis, the "rate-adjustment capacity determination" method has been considered

$$\mathrm{SOH} = \frac{X_a K_c}{X_t} 100 \tag{20}$$

TABLE II
ESTIMATION OF PRESENT SOH FOR BATTERY 1

Method	Actual Capacity Estimation (Ah)	SOH Estimation (%)
IEEE 1188-2005	5.8	81.2
EKF	6.0	83.0
Proposed method	5.9	82.7

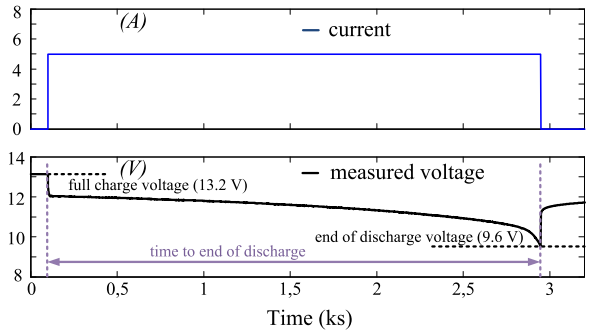

Fig. 6. IEEE 1188-2005 experimental tests performed for battery 1, VRLA 12 V 7.2 Ah. $X_a = 5$ A, $X_t = 6.5$ A, $K_c = 1.056$, working temperature 20 °C.

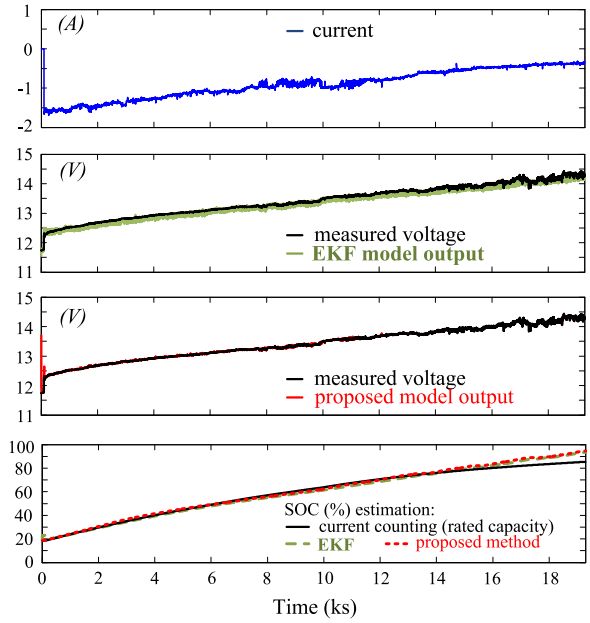

Fig. 7. Experimental tests performed with battery 1, VRLA 12 V 7.2 Ah, working temperature 20 °C. Comparison between EKF and proposed method used for SOC estimation during charge operation performed by a professional charger device. Estimated SOH is about 80% in both cases.

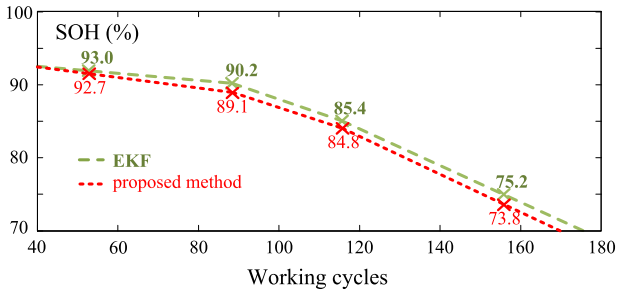

Fig. 8. Experimental tests performed with battery 1, VRLA 12 V 7.2 Ah. Comparison between EKF and proposed method in SOH estimation during accelerated ageing tests. Each working cycle includes a complete discharge (depth of discharge is 100%) and a full recharge. Working temperature is 20 °C.

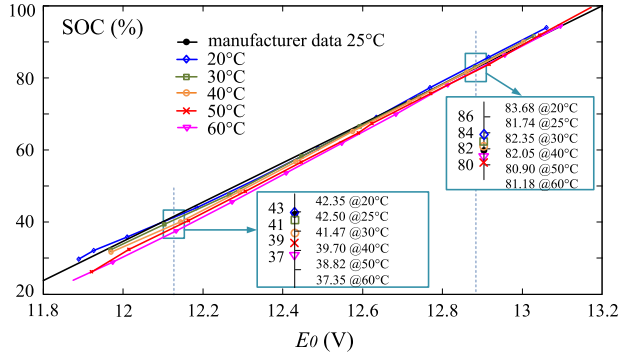

Fig. 9. Experimental tests performed with battery 1, VRLA 12 V 7.2 Ah. SOC(E_0) curve is extrapolated at different temperatures; also, the curve provided by manufacturer is reported (25 °C). SOC deviation due to temperature effect is highlighted considering both high and low SOC levels.

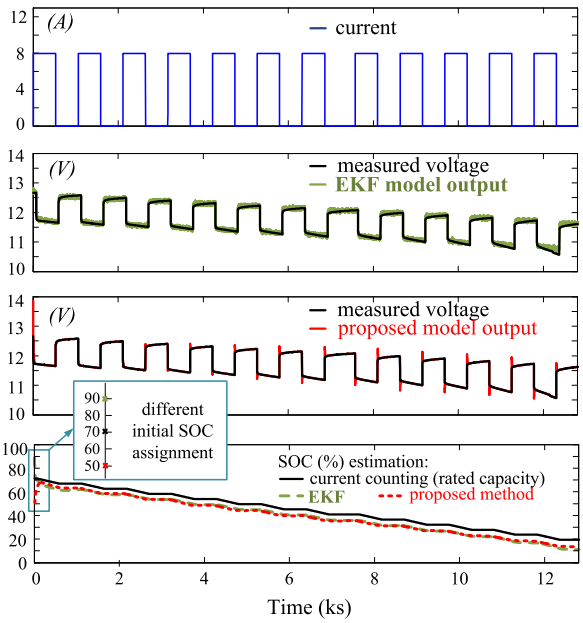

Fig. 10. Experimental tests performed with battery 2, VRLA 12 V 27 Ah, working temperature 25 °C. Comparison between EKF and proposed method used for SOC estimation during discharge operation. Estimated SOH is about 92% in both cases. Different initial SOC values are assigned: 70.6% for current counting method, 89% for EKF, and 50% for the proposed method.

where X_a is the actual current rate used for the test, X_t is the rated one, and K_c is the temperature correction factor.

Fig. 7 deals with the results obtained for battery 1 considering a real operating situation when the charge process is performed by a charger device specifically designed for intermediate-size VRLA batteries. It is confirmed that the proposed method is able to carry out an accurate estimation of the ESS state even in this practical case.

In order to evaluate the proposed method capability to model variation of SOH during lifetime, several accelerated ageing tests have been performed by continuously repeating a wide number of working cycles. Each working cycle includes a complete discharge (depth of discharge is 100%) and a full recharge. Temperature is maintained at 20 °C (see Fig. 8).

The effects of ambient temperature have been pointed out by the following test. Several SOC(E_0) curves have been collected at different temperatures (20–60 °C) by means of a climate chamber and some temperature sensors. The results are shown in Fig. 9. Two different regions of these curves have been highlighted in order to show the temperature effects at low and high SOC values. It is worth noting that, while SOC variations at high SOC values are limited to 2%–3% and could be considered negligible in many applications, the response is different at low SOC levels. Therefore, a compensation is strictly recommended in this operating region due to significant temperature dependence. In order to consider such an effect, the information of Fig. 9 has been included in the look-up table SOC(E_0) of Fig. 2.

Figs. 10–12 show other experimental results obtained with batteries having different technology and size, addressing different operating scenarios.

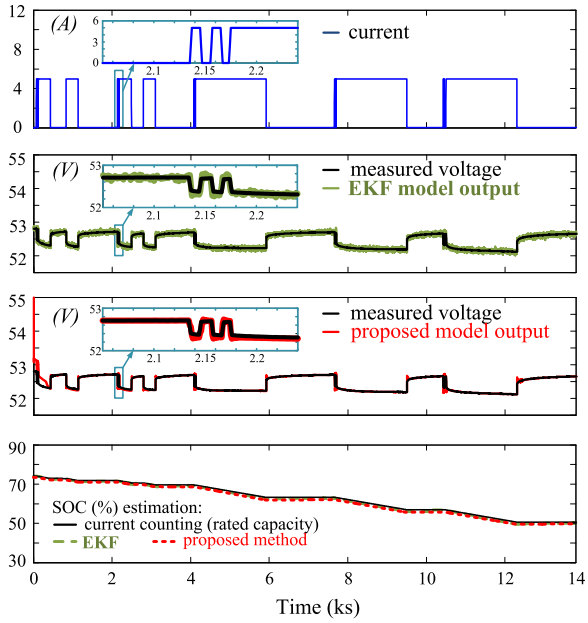

Fig. 11. Experimental tests performed with battery 3, Li-ion 51.2 V 40 Ah, working temperature 25 °C. Comparison between EKF and proposed method used for SOC estimation during discharge operation. Estimated SOH is about 97% in both cases. In the zoom windows, it is highlighted the waveform of model output during fast transients.

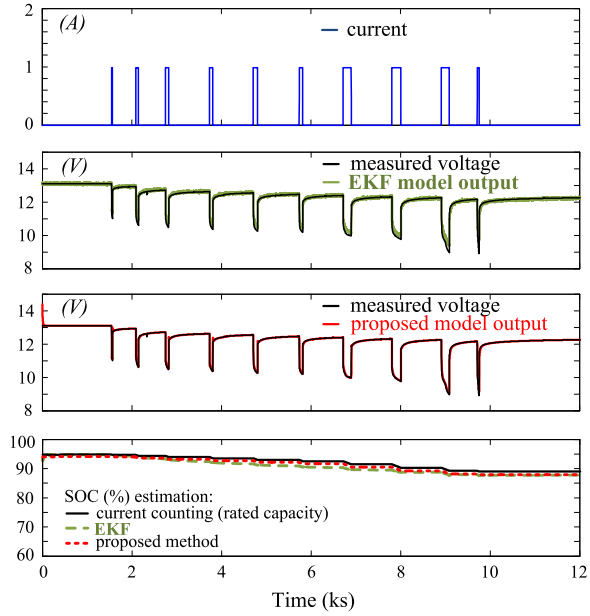

Fig. 12. Experimental tests performed with battery 4, Ni-MH 12 V 4.8 Ah, working temperature 25 °C. Comparison between EKF and proposed method used for SOC estimation during discharge operation. Estimated SOH is about 98% in both cases.

Fig. 10 shows a pulsed discharge for battery 2, where random SOC values have been assigned to initialize the estimation methods. The results confirm the effectiveness of the proposed method in the cases of unknown or wrong initial SOC value. As a matter of fact, the convergence to final value is obtained after an acceptable settling time.

Fig. 11 deals with battery 3 whose electrochemical technology is $LiFePO_4$. In such a case, the $E_0(V_{SOC})$ relationship is no longer linear, but its waveform can be easily divided into several periods, where each segment can be considered linear [54]. The model response during fast transients has been highlighted using zoomed windows. The proposed method is also able to track the real voltage while providing an accurate SOC estimation. If the current pulse repetition frequency increases to values outside design specifications, PI gains should be settled again by means of a simple fine-tuning. On the contrary, the other estimation methods could involve more complicated setting procedures, for example, as reported for EKF in [51].

The proposed method has been also used for Ni-MH batteries and the effectiveness is again verified, as the results shown in Fig. 12 confirm.

IV. Conclusion

In many applications dealing with electrical energy storage, a key point in the management of electrochemical batteries is the widening of both energy capability and lifetime. Accurate modeling of ESS is essential since it allows to optimize control strategy in power electronics systems.

In this paper, a review has been performed concerning both equivalent circuits to model ESS and methods to estimate SOC and SOH. From this background, a novel technique for ESS state estimation has been developed. It is devoted to main electrochemical technologies. The method mainly consists of a PI-based observer scheme, in which SOC and SOH values are determined by a suitable algorithm. PIs elaborates data provided by a real-time comparison between the measured ESS voltage and its calculated value determined by an improved extended runtime circuit model. The result of such a comparison is used to suitably tune the main parameters of the ESS circuit model, in order to compensate for inaccuracies related to measurement, variable environmental conditions, and so on. Moreover, a simple start-up identification procedure is necessary. Some of the advantages of the proposed method are accuracy, real-time SOC and SOH estimation capability, as well as model compliance for several applications involving ESS.

Finally, the proposed approach can be considered a good tradeoff between desired accuracy and complexity of the estimation algorithm while avoiding the time-consuming procedures implemented by other methods. Comprehensive experimental tests confirm the adaptability of the algorithm to a wide number of real applications and also in a number of different operating conditions.

References

[1] P. C. Loh, D. Li, Y. K. Chai, and F. Blaabjerg, "Hybrid AC–DC microgrids with energy storages and progressive energy flow tuning," *IEEE Trans. Power Electron.*, vol. 28, no. 4, pp. 1533–1543, Apr. 2013.

[2] S. Huang, B. Huang, and F. Pai, "Fast charge strategy based on the characterization and evaluation of LiFePO4 batteries," *IEEE Trans. Power Electron.*, vol. 28, no. 4, pp. 1555–1562, Apr. 2013.

[3] M. Cugnet, M. Dubarry, and B. Lyaw, "Secondary batteries—Lead-acid systems—Modeling," in *Reference Module in Chemistry, Molecular Sciences and Chemical Engineering Encyclopedia of Electrochemical Power Sources*. New York, NY, USA: Elsevier, 2009, pp. 816–828.

[4] C. Zhang, K. Li, S. Mcloone, and Z. Yang, "Battery modelling methods for electric vehicles—A review," in *Proc. 2014 IEEE Eur. Control Conf.*, pp. 2673–2678.

[5] A. Hussein and I. Batarseh, "An Overview of generic battery models," in *Proc. 2011 IEEE Power Energy Soc. Gen. Meeting*, pp. 1–6.

[6] A. Seaman, T. Dao, and J. McPhee, "A survey of mathematical-based equivalent-circuit and electrochemical battery models for hybrid and electric vehicle simulation," *J. Power Sources*, vol. 256, pp. 410–423, Jun. 2014.

[7] S. M. Mousavi and M. Nikdel, "Various battery models for various simulation studies and applications," in *Renewable and Sustainable Energy Reviews*, vol. 32. New York, NY, USA: Elsevier, Apr. 2014, pp. 477–485.

[8] G. Brando, A. Dannier, I. Spina, and L. Piegari, "Comparison of accuracy of different LiFePO4 battery circuital models," in *Proc. 2014 IEEE Power Electron. Elect. Drives, Autom. Motion Int. Symp.*, pp. 1092–1097.

[9] S. Kai and S. Qifang, "Overview of the types of battery models," in *Proc. 2011 IEEE 30th Chin. Control Conf.*, pp. 3644–3648.

[10] N. Achaibou, M. Haddadi, and A. Malek, "Lead acid batteries simulation including experimental validation," *J. Power Sources*, vol. 185, no. 2, pp. 1484–1491, Dec. 2008.

[11] H. He, R. Xiong, H. Guo, and S. Li, "Comparison study on the battery models used for the energy management of batteries in electric vehicles," in *Energy Conversion and Management, vol. 64*. New York, NY, USA: Elsevier, Dec. 2012, pp. 113–121.

[12] C. M. Sheperd, "Design of primary and secondary cells—Part II. An equation describing battery discharge," *J. Electrochem. Soc.*, vol. 112, no. 7, pp. 657–664, Jul. 1965.

[13] R. S. Treptow, "The lead-acid battery: Its voltage in theory and practice," *J. Chem. Edu.*, vol. 79, no. 3, Mar. 2002.

[14] N. Kularatna, "Dynamics and modeling of rechargeable batteries," *IEEE Power Electron. Mag.*, vol. 1, no. 4, pp. 23–33, Dec. 2014.

[15] M. Einhorn, F. V. Conte, C. Kral, and J. Fleig, "Comparison, selection, and parameterization of electrical battery models for automotive applications," *IEEE Trans. Power Electron.*, vol. 28, no. 3, pp. 1429–1437, Mar. 2013.

[16] B. Schweighofer, K. Raab, and G. Brasseur, "Modeling of high power automotive batteries by the use of an automated test system," *IEEE Trans. Instrum. Meas.*, vol. 52, no. 4, pp. 1087–1091, Aug. 2003.

[17] J. Li and M. Mazzola, "Accurate battery pack modeling for automotive applications," *J. Power Sources,* Sep. 2013, vol. 237, pp. 215–228.

[18] W. Wang, H. Chung, and J. Zhang, "Near-real-time parameter estimation of an electrical battery model with multiple time constants and soc-dependent capacitance," *IEEE Trans. Power Electron.*, vol. 29, no. 11, pp. 5905–5920, Nov. 2014.

[19] L. Benini, G. Castelli, A. Macii, E. Macii, M. Poncino, and R. Scarsi "Discrete-time battery models for system-level low-power design," *IEEE Trans. Very Large Scale Integr. Syst.*, vol. 9, no. 5, pp. 630–640, Oct. 2001.

[20] S. Gold, "A PSPICE macromodel for lithium-ion batteries," in *Proc. 1997 IEEE Battery Appl. Advances Conf.*, pp. 215–222.

[21] M. Chen and A. Rincon-Mora, "Accurate electrical battery model capable of predicting runtime and I–V performance," *IEEE Trans. Energy Convers.*, vol. 21, no. 2, pp. 504–511, Jun. 2006.

[22] R. Kroeze and P. Krein, "Electrical battery model for use in dynamic electric vehicle simulations," in *Proc. 2008 IEEE Power Electron. Spec. Conf.*, pp. 1336–1342.

[23] O. Tremblay and L. Dessaint, "Experimental validation of a battery dynamic model for EV applications," *World Elect. Veh. J.*, vol. 3, pp. 1–10, May 2009.

[24] S. Li and B. Ke, "Study of battery modeling using mathematical and circuit oriented approaches," in *Proc. 2011 IEEE Power Energy Soc. Gen. Meeting*, pp. 1–8.

[25] R. A. Jackey, "A simple, effective lead-acid battery modeling process for electrical system component selection," paper presented at the 2007 SAE World Congr. Exhib., Warrendale, PA, USA, Paper 2007-01-0778.

[26] B. S. Bhangu, C. M. Bingham, D. A. Stone, and P. Bentley, "Observer techniques for estimating the SOC and SOH of VRLABs for hybrid electric vehicles," in *Proc. 2005 IEEE Veh. Power Propulsion Conf.*, pp. 780–789.

[27] B. S. Bhangu, C. M. Bingham, D. A. Stone, and P. Bentley, "Nonlinear observer techniques for prediction state-of-charge and state-of-health of lead-acid batteries for hybrid-electric vehicles," *IEEE Trans. Veh. Technol.*, vol. 54, no. 3, pp. 783–794, May 2005.

[28] C. R. Gould, C. M. Bingham, D. A. Stone, and P. Bentley, "Battery health determination by subspace parameter estimation and sliding mode control for an all-electric personal rapid transit vehicle the ULTra," in *Proc. 2008 IEEE Power Electron. Spec. Conf.*, pp. 4381–4385.

[29] C. R. Gould, C. M. Bingham, D. A. Stone, and P. Bentley, "Novel battery model of an all-electric personal rapid transit vehicle to determine state-of-health through subspace parameter estimation and a Kalman estimator," in *Proc. 2008 IEEE Power Electron. Elect. Drives, Autom. Motion Int. Symp.*, pp. 1217–1222.

[30] A. Salkind, P. Singh, A. Cannone, T. Atwater, X. Wang, and D. Reisner, "Impedance modeling of intermediate size lead-acid batteries," *J. Power Sources*, vol. 116, pp. 174–184, Jul. 2003.

[31] D. I. Stroe, M. Swierczynski, A. I. Stroe, V. Knap, R. Teodorescu, and S. J. Andreasen, "Evaluation of different methods for measuring the impedance of lithium-ion batteries during ageing," in *Proc. 2005 IEEE Ecological Vehicles Renewable Energies Int. Conf.*, pp. 1–8.

[32] H. Wang, G. Li, M. Li, Z. Jiang, X. Wang, and Q. Zhao, "Third-order dynamic model of a lead acid battery for use in fuel cell vehicle simulation," in *Proc. 2011 IEEE Mechatron. Sci. Elect. Eng. Comput. Conf.*, pp. 715–720.

[33] M. Ceraolo, "New dynamical models of lead-acid batteries," *IEEE Trans. Power Syst.*, vol. 15, no. 4, pp. 1184–1190, Nov. 2000.

[34] H. Wenzl, "Self-discharge," *Reference Module in Chemistry, Molecular Sciences and Chemical Engineering Encyclopedia of Electrochemical Power Sources*. New York, NY, USA: Elsevier, 2009, pp. 407–412.

[35] D. Doerffel and S. A. Sharkh, "A critical review of using the Peukert equation for determining the remaining capacity of lead-acid and lithium-ion batteries," *J. Power Sources*, vol. 155, no. 2, pp. 395–400, Apr. 2006.

[36] S. M. Mousavi, S. H. Fathi, and G. H. Riahi, "Energy management of wind/PV and battery hybrid system with consideration of memory effect in battery," in *Proc. 2009 IEEE Clean Elect. Power Int. Conf.*, pp. 630–633.

[37] A. I. Stan, M. Swierczynski, D. I. Stroe, R. Teodorescu, S. J. Andreasen, and K. Moth, "A comparative study of lithium ion to lead acid batteries for use in UPS applications," in *Proc. 2014 IEEE Int. Telecommun. Energy Conf.*, pp. 1–8.

[38] M. Coleman, W. G. Hurley, and C. K. Lee, "An improved battery characterization method using a two-pulse load test," *IEEE Trans. Energy Convers.*, vol. 23, no. 2, pp. 708–713, Jun. 2008.

[39] W. Waag and D. U. Sauer, "State-of-charge/health," *Reference Module in Chemistry, Molecular Sciences and Chemical Engineering Encyclopedia of Electrochemical Power Sources*. New York, NY, USA: Elsevier, 2009, pp. 793–804.

[40] W. Chang, "The state of charge estimating methods for battery: A review," in *International Scholarly Research Notices Applied Mathematics*, New York, NY, USA: Hindawi, 2013, vol. 2013, pp. 1–8.

[41] IEEE Recommended Practice for Maintenance, Testing and Replacement of Valve-Regulated Lead-Acid (VRLA) Batteries for Stationary Applications, *IEEE Standard 1188-2005*, Feb. 2006.

[42] IEEE Recommended Practice for Maintenance, Testing and Replacement of Valve-Regulated Lead-Acid (VRLA) Batteries for Stationary Applications—Amendment 1: Updated VRLA Maintenance Considerations, *IEEE Standard 1188a-2014*, Jul. 2014.

[43] B. Pattipati, B. Balasingam, G. V. Avvari, K. R. Pattipati, and Y. Bar-Shalom, "Open circuit voltage characterization of lithium-ion batteries," *J. Power Sources*, vol. 269, pp. 317–333, Dec. 2014.

[44] M. Coleman, C. K. Lee, C. Zhu, and W. G. Hurley, "State-of-charge determination from EMF voltage estimation using impedance, terminal voltage and current for lead-acid and lithium ion batteries," *IEEE Trans. Ind. Electron.*, vol. 54, no. 5, pp. 2550–2557, Aug. 2007.

[45] P. E. Pascoe and A. H. Anbuky, "VRLA battery discharge reserve time estimation," *IEEE Trans. Power Electron.*, vol. 19, no. 6, pp. 1515–1522, Nov. 2004.

[46] J. Kalawoun, K. Biletska, F. Suard, and M. Montaru, "From a novel classification of the battery state of charge estimators toward a conception of an ideal one," *J. Power Sources*, vol. 279, pp. 694–706, Apr. 2015.

[47] F. Huet, "A review of impedance measurements for determination of the state-of-charge or state-of-health of secondary batteries," *J. Power Sources*, vol. 70, no. 1, pp. 59–69, Jan. 1998.

[48] W. Waag, C. Fleischer, and D. U. Sauer, "Critical review of the methods for monitoring of lithium-ion batteries in electric and hybrid vehicles," *J. Power Sources*, vol. 258, pp. 321–339, Jul. 2014.

[49] P. D. Zimmerman, D. E. Zimmerman, and G. L. Claypoole, "Apparatus and method for testing remaining capacity of a battery," U.S. Patent 6 823 274, Nov. 2004.

[50] R. E. Kalman, "A new approach to linear filtering and prediction problems," *Trans. ASME J. Basic Eng. Ser. D*, New York, NY, USA, pp. 35–45, 1982.

[51] J. Kim, S. Lee, and B. H. Cho, "Complementary cooperation algorithm based on DEKF combined with pattern recognition for SOC/capacity

estimation and SOH prediction," *IEEE Trans. Power Electron.*, vol. 27, no. 1, pp. 436–451, Jan. 2012.
[52] M. Gholizadeh and F. R. Salmasi, "Estimation of state of charge, unknown nonlinearities, and state of health of a lithium-ion battery based on a comprehensive unobservable model," *IEEE Trans. Ind. Electron.*, vol. 61, no. 3, pp. 1335–1344, Mar. 2014.
[53] A. Lievre, S. Pellissier, A. Sari, P. Venet, and A. Hijazi, "Luenberger observer for SoC determination of lithium-ion cells in mild hybrid vehicles compared to a Kalman filter," in *Proc. 2015 IEEE Ecol. Veh. Renewable Energies Int. Conf.*, pp. 1–7.
[54] J. Xu, C. C. Mi, B. Cao, J. Deng, Z. Chen, and S. Li, "The state of charge estimation of lithium-ion batteries based on a proportional-integral observer," *IEEE Trans. Veh. Technol.*, vol. 63, no. 4, pp. 1614–1621, May 2014.
[55] X. Tang, Y. Wang, and Z. Chen, "A method for state-of-charge estimation of LiFePO4 batteries based on a dual-circuit state observer," *J. Power Sources*, vol. 296, pp. 23–29, Nov. 2015.
[56] X. Chen, W. Shen, Z. Cao, and A. Kapoor, "A comparative study of observer design techniques for state of charge estimation in electric vehicles," in *Proc. 2012 IEEE Ind. Electron. Appl. Conf.*, pp. 102–107.
[57] F. Codecà, S. M. Savaresi, and G. Rizzoni, "On battery state of charge estimation: A new mixed algorithm," in *Proc. 2008 IEEE Control Appl. Int. Conf.*, pp. 102–107.
[58] F. Codecà, S. M. Savaresi, and V. Manzoni, "The mix estimation algorithm for battery state-of-charge estimator—Analysis of the sensitivity to measurement errors," in *Proc. 2009 IEEE Decision Control Chin. Control Conf.*, pp. 8083–8088.
[59] S. Sato and A. Kawamura, "A new estimation method of state of charge using terminal voltage and internal resistance for lead acid battery," in *Proc. 2002 IEEE Power Convers. Conf.*, pp. 565–570.
[60] S. Tong, M. P. Klein, and J. W. Park, "On-line optimization of battery open circuit voltage for improved state-of-charge and state-of-health estimation," *J. Power Sources*, vol. 293, pp. 416–428, Oct. 2015.
[61] X. Hu, S. Li, and H. Peng, "A comparative study of equivalent circuit models for Li-ion batteries," *J. Power Sources*, vol. 198, pp. 359–367, Jan. 2012.

Mario Cacciato (S'99–M'00) received the M.S. degree in electrical engineering (*cum laude*) from the University of Catania, Catania, Italy, in 1996, and the Ph.D. degree in electronic engineering from the University of Reggio Calabria, Reggio Calabria, Italy, in 2000.

In the same year, he became an Assistant Professor with the Department of Electrical Engineering, Sapienza University of Rome, Rome, Italy. In 2004, he was with the Department of Electrical, Electronics, and Computer Engineering, University of Catania, where since 2011, he has been an Associate Professor with the Department of Electrical and Electronic Engineering and Informatics, where he is currently involved in teaching courses on electrical machines. He is the author or coauthor of more than 100 technical papers published in journals and proceedings of international conferences. His current research interests include power electronics, control of electric drives, electromagnetic compatibility, renewable energy, and hydrogen applications.

Prof. Cacciato is a Member of the IEEE Industrial Electronics and the IEEE Power Electronics Societies. He is also a Member of the European Power Electronics Association (EPE), where he is currently the Member of the EPE Executive Council. He is the Chair of the EPE Chapter on Solar Energy.

Giovanni Nobile received the B.S. and M.S degrees in electrical engineering from the University of Catania, Catania, Italy, in 2005 and 2007, respectively.

In 2007, he joined some international companies where he was involved in the field of power generation from renewables working on plant design, high-voltage equipment, grid connection infrastructures, monitoring systems, operation and maintenance. He is currently a Research Fellow with the Department of Electric, Electronic and Computer Science, University of Catania. His current research interests include energy storage systems, renewable energy power plants, power electronics and electric drives.

Dr. Nobile is a Member of the Italian Association of Electrical and Electronics Engineers (AEIT).

Giuseppe Scarcella (S'98–M'99) received the M.S. and Ph.D. degrees in electrical engineering from the University of Catania, Catania, Italy, in 1995 and 1999, respectively.

In 1998, he spent a period at the University of Wisconsin–Madison, Madison, WI, USA, working on sensorless control of electrical drives. In 1999, he joined the Department of Electrical, Electronic, and Systems Engineering, University of Catania, as a Temporary Researcher. In 2001, he obtained a permanent position as an Assistant Professor, in the same department, where, since 2005, he has been an Associate Professor in the areas of power electronics and electrical machines and drives. He is the author or coauthor of over 130 technical papers published in journals and proceedings of national and international conferences and is a holder of several international patents. His current research interests include sensorless control of electrical machines, advanced control, digital modulation techniques, efficiency optimization techniques, and electromagnetic compatibility.

Prof. Scarcella is currently an Associate Editor for the IEEE TRANSACTIONS ON INDUSTRY APPLICATIONS. He has received the Third Prize for a paper he presented at the IEEE Industry Applications Society (IAS) Annual Meeting in 1998 and an Award for the best paper published in the IEEE TRANSACTIONS ON POWER ELECTRONICS in 2000. He also received an SGS Thomson (now ST Microelectronics) Research Grant in 1995. He is a Member of the IEEE Industry Applications Society.

Giacomo Scelba (S'04–M'07) received the M.S. and Ph.D. degrees in electrical engineering from the University of Catania, Catania, Italy, in 2002 and 2005, respectively.

He is currently an Assistant Professor with the Department of Electric, Electronic and Computer Science, University of Catania. His current research interests include sensorless control, digital signal processing, ac drive control technologies, fault-tolerant control solutions devoted to multiphase and multidrive ac systems, and control techniques for renewable energy systems.

Dr. Scelba is currently an Associate Editor for the IEEE TRANSACTIONS ON INDUSTRY APPLICATIONS. He is a Member of the IEEE Industry Applications, the IEEE Industrial Electronics, and the IEEE Power Electronics Societies and is a Registered Professional Engineer in Italy.